Electron energy structure of self-assembled In(Ga)As nanostructures probed by capacitance-voltage spectroscopy and one-dimensional numerical simulation

Wen Lei[a)]

Department of Electronic Materials Engineering, Research School of Physical Sciences and Engineering, The Australian National University, Canberra ACT 0200, Australia; and Department of Physics and CeNIDE, Universität Duisburg-Essen, D-47048 Duisburg, Germany

Christian Notthoff, Matthias Offer, Cedrik Meier, and Axel Lorke

Department of Physics and CeNIDE, Universität Duisburg-Essen, D-47048 Duisburg, Germany

Chennupati Jagadish

Department of Electronic Materials Engineering, Research School of Physical Sciences and Engineering, The Australian National University, Canberra ACT 0200, Australia

Andreas D. Wieck

Solid State Physics, Ruhr-Universität Bochum, D-44780 Bochum, Germany

(Received 29 September 2008; accepted 5 December 2008)

The electron energy structure of self-assembled In(Ga)As/GaAs nanostructures, quantum dots, and quantum rings was studied with capacitance-voltage spectroscopy and one-dimensional numerical simulation using Poisson/Schrödinger equations. The electron energy levels in the quantum dots and quantum rings with respect to the electron ground state of the wetting layer were determined directly from capacitance-voltage measurements with a linear lever arm approximation. In the regime where the linear lever arm approximation was not valid anymore (after the charging of the wetting layer), the energy difference between the electron ground state of the wetting layer and the GaAs conduction band edge was obtained indirectly from a numerical simulation of the conduction band under different gate voltages, which led to the erection of complete electron energy levels of the nanostructures in the conduction band.

I. INTRODUCTION

Recently, much attention has been devoted to investigating self-assembled nanostructures, such as quantum dots (QDs) and quantum rings (QRs), due to their great potential in device applications.[1,2] To further improve device performance, it is important to know the energy structure of these nanostructures. Much work has been done to resolve the electronic structure of these nanostructures theoretically.[3–8] Experimentally, the electronic structure of these nanostructures can be assessed by optical and transport measurements. Some experimental work has also been done to understand the electronic structure of QDs and QRs by using photoluminescence and photoluminescence excitation spectroscopy, photocurrent spectroscopy, capacitance-voltage (C-V) spectroscopy, and absorption spectroscopy, among other methods.[2,9–17] As for the use of C-V spectroscopy to determine absolute energy scales, one problem is to determine the Schottky barrier formed on the sample surface. There are two possible ways to do it: one way is to use a reference sample to extract the Schottky barrier, in which no QD (or QR) layer is present; the other way is to fabricate several devices with different geometric lever arms to extract the Schottky barrier.[16,17]

In this work, we demonstrate that the electron energy levels in QDs and QRs with respect to the GaAs conduction band edge can be easily obtained through C-V measurements in combination with a 1D-Poisson/Schrödinger simulation of the conduction band under different gate voltages.

II. EXPERIMENTAL DETAILS

Both the QD and QR samples were grown on a semi-insulating (001) GaAs substrate in a solid-source molecular-beam epitaxy (MBE) system. The active part of the QD sample was grown in the following layer

[a)]Address all correspondence to this author.
e-mail: wen.lei@anu.edu.au

This paper was selected as an Outstanding Symposium Paper for the 2008 International Materials Research Conference, Symposium D. To maintain *JMR*'s rigorous, unbiased peer review standards, the *JMR* Principal Editor and reviewers were not made aware of the paper's designation as Outstanding Symposium Paper.
DOI: 10.1557/JMR.2009.0293

© 2009 Materials Research Society

sequence: first a 20 nm heavily Si-doped GaAs back contact layer, then a 42.5 nm undoped GaAs tunneling barrier layer, then a 5 monolayer (ML) InAs QD layer, then a 30 nm GaAs, and 54 periods of AlAs (3 nm)/GaAs (1 nm) superlattice as the blocking layer, then a 10 nm GaAs cap layer, and then a 5 ML InAs QD layer [for atomic force microscopy (AFM) imaging]. The active part of the QR sample was grown in a similar sequence. It was composed of a 60 nm heavily Si-doped GaAs (back contact) layer, a 25 nm undoped GaAs tunneling barrier, 1.4–1.7 ML In(Ga)As for the QR layer (the detailed growth of QRs: first 1.4–1.7 ML InAs was deposited at 585 °C to form QDs, then the QDs were capped by 2 nm GaAs at 545 °C, after that a 30 s growth interruption was introduced; the growth time for the 1.4–1.7 ML InAs and 2 nm GaAs layer are 4 and 9.9 s, respectively, and the As_2 pressure is kept at 7.9×10^{-8} Torr during the growth), a 30 nm GaAs spacer, 34 periods of an AlAs (3 nm)/GaAs (1 nm) superlattice as a blocking layer, a 5 nm GaAs cap layer, and 1.4–1.7 ML In(Ga)As QR layer (for AFM imaging). The n^+-doped GaAs back contact layers were contacted from the sample surface by an AuGe alloy annealed at T = 450 °C and subsequently, the NiCr Schottky gate electrodes were prepared. C-V spectra of the sample were measured by superimposing a DC gate bias (V_g) with a small AC voltage (5 mV rms) of variable frequency (f). In the C-V measurements, the standard lock-in technique was used to record the capacitance signal. Whenever the chemical potential of the back contact (Fermi energy) is in resonance with either the discrete energy levels in the InAs QDs and QRs, or the InAs wetting layer (WL), or the two-dimensional electron gas (2DEG) formed at the interface between the intrinsic GaAs region and the AlAs/GaAs superlattice, resonant tunneling occurs and the capacitance signal shows characteristic peaks.[12–17] All the C-V measurements were made at 4.2 K. All C-V measurements demonstrated reasonable uniformity over different areas of the wafer.

III. RESULTS AND DISCUSSION

A. Electron energy structure of InAs/GaAs QDs

A schematic profile of the conduction band edge of the samples is shown in Fig. 1. The structure parameters l_1, l_2, and l_0 in Fig. 1 are the distance from the back contact to the QD (QR) layer, 2DEG, and sample surface, respectively. E_1 and E_2 in Fig. 1 represent the energy difference between the Fermi energy level and the GaAs conduction band edge at the position of the QD (QR) layer and the 2DEG, respectively.

A typical C-V spectrum of the QD sample taken at f = 83 Hz and the second derivative of the C-V trace are shown in Fig. 2(a). The inset of Fig. 2(a) shows the typical AFM image of the surface of the QD sample. It is observed that InAs QDs are formed in the sample with a mean height and diameter of about 7.5 nm and

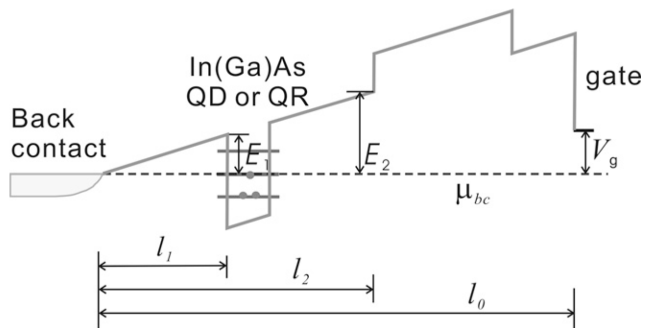

FIG. 1. Schematic profile of conduction band of the samples. The parameters l_0, l_1, and l_2 are 298.5 (196), 42.5 (25), and 72.5 (55) nm for the QD (QR) sample, respectively.

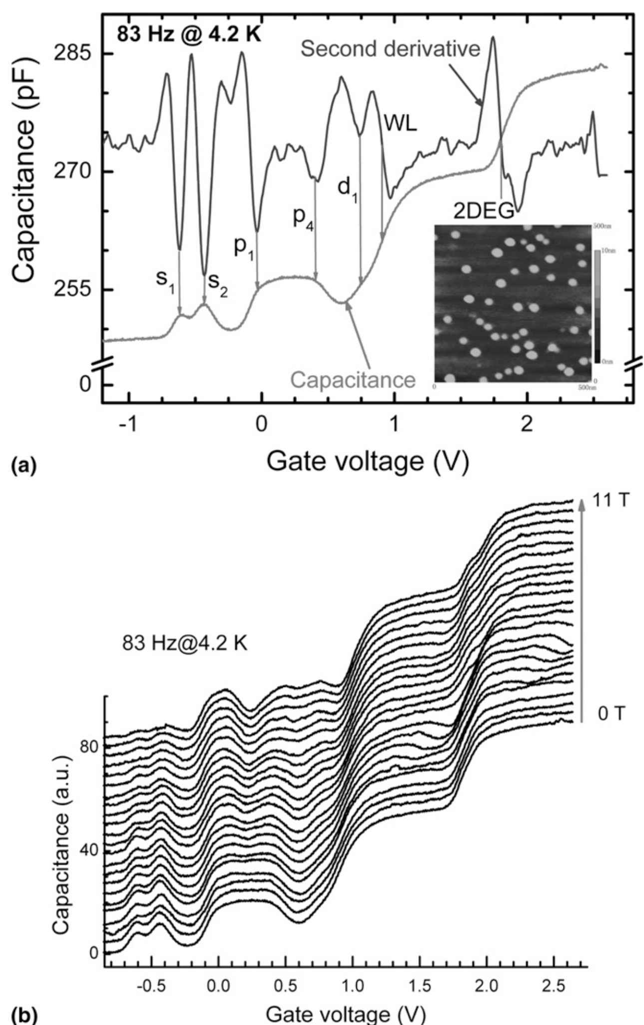

FIG. 2. (a) Typical C-V spectrum and its second derivative and (b) C-V spectra of the QD sample taken with f = 83 Hz at different perpendicular magnetic fields, which range from 0 T to 11 T with an interval of 0.5 T. The arrows in (a) mark the positions of the charging events. The inset of (a) shows the typical AFM image of the sample surface.

23 nm, respectively. Obviously, at least seven charging features can be observed, which are labeled as s_1 (–0.62 V), s_2 (–0.43 V), p_1 (–0.04 V), p_4 (0.4 V), d_1 (0.74 V), WL (0.9 V), and 2DEG (1.8 V) in Fig. 2(a), respectively. To extract the origin of these charging features, C-V measurements of the QD sample are performed at different perpendicular magnetic fields, ranging from 0 T to 11 T with an interval of 0.5 T. Figure 2(b) shows the C-V spectra of the sample taken at different perpendicular magnetic fields with f = 83 Hz. According to the energy dispersion of these charging features,[18,19] the charging peaks labeled as s_1 and s_2 can be attributed to loading of the first and second electron into *s*-like states of the QDs. The charging peaks labeled as p_1 and p_4 can be ascribed to loading of the third and sixth electron into *p*-like states in the QDs. Because of the limited spectroscopic resolution, the *C-V* signal associated with charging of the fourth and fifth electron state cannot be clearly separated from the features p_1 and p_4 in Fig. 2(a), and they appear as a broad charging peaks, ranging from –0.24 V to 0.6 V. In the same manner, the charging features labeled as d_1, WL, and 2DEG can be attributed to the loading of electrons into *d*-like states in QDs, InAs WL, and 2DEG, respectively.[16–19] It should be noted that the onset voltage of the charging features in the CV spectra here is about 200–300 meV higher than those reported by other researchers.[17,19] However, since in the following we do not use the absolute values of the gate voltages (only gate voltage differences), this shift of the V_g scale does not affect our results.

Because of the low QD density ($\sim 8 \times 10^9$ cm^{-2}) grown in the sample, it is reasonable to assume that the charge accumulated in the QDs is not sufficient to pin the conduction band. Thus, the linear lever arm approximation ($\Delta E = e\Delta Vg/\lambda$, with the lever arm $\lambda = l_0/l_1$) can be used up to the onset of the charging of InAs WL to convert charging voltages into charging energies.[12,13,19,20] By using this linear lever arm approximation, the energy difference between the electron ground state in the InAs QDs and the electron ground state in the InAs WL is determined to be ~216 meV. Further, according to the charging voltage difference between s_1 and s_2, the electron Coulomb blockade energy E^{C}_{ss} for the QDs is extracted to be 27 meV. For the energy difference between s_1 and p_1, a value of 82 meV is found. Theoretically, the energy difference between the loading of the first electron and the third electron into the QD is estimated to be $\Delta E_{(s_1 \rightarrow p_1)} = \hbar\omega + \frac{5}{4}E^{C}_{ss}$.[19] By using the electron Coulomb blockade energy E^{C}_{ss} determined above, the quantization energy ($\hbar\omega$) in the QDs is found to be ~48 meV.

After the charging of WL, there is a lot of charge accumulated in the WL, which pins the conduction band and makes the above linear lever arm approximation invalid. The influence of charge accumulated in the WL on the conduction band of the sample can be simulated with the software 1D Poisson/Schrödinger.[21] The Schottky barrier on the sample surface and the Si-doping concentration in the back contact are assumed to be 0.6 eV and 1×10^{18} cm^{-3}, respectively. Further, a 1.2 nm $In_{0.26}Ga_{0.74}As$ layer is used to represent the InAs WL in the simulation. (The value of 1.2 nm $In_{0.26}Ga_{0.74}As$ as the InAs wetting layer was chosen to reproduce the 0.9 V gate voltage difference between the onset of the charging of the wetting layer and that of the 2DEG in the 1D Poisson/Schrödinger simulation.) To see the onset of the charging of WL and 2DEG, a series of gate voltages (from −0.6 V to 1.4 V) is applied on the sample structure in the simulation. Figure 3 shows the conduction band and the carrier distribution in the sample, simulated under different gate voltages. It is observed that the loading of electrons into WL and 2DEG occurs at 0.2 V and 1.1 V, respectively. The voltage difference (0.9 V) between the onset of charging of WL and 2DEG simulated is the same as that determined from CV

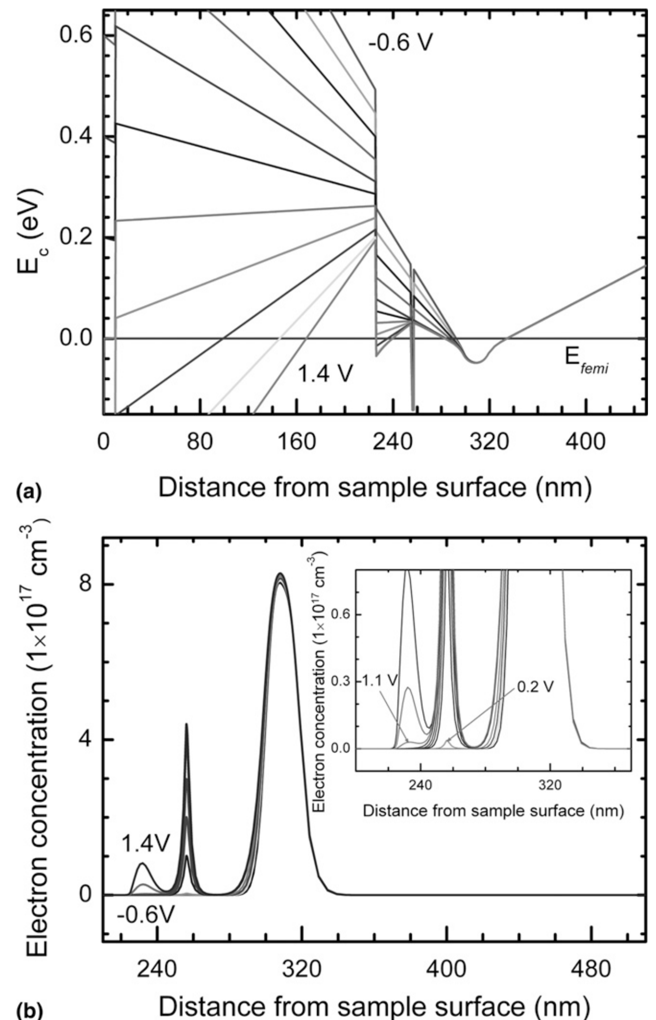

FIG. 3. (a) Calculated conduction band and (b) electron concentration distribution in the sample, for different gate voltages. The inset of (b) shows an expanded view of the results.

measurements, indicating that the 1.2 nm $In_{0.26}Ga_{0.74}As$ layer works well as the InAs WL in the simulation.

Figure 4 shows the values of E_1 and E_2, simulated with different gate voltages. It should be noted that the spatial position of the 2DEG is not exactly at the GaAs/AlGaAs interface in the simulation, but 6 nm from the GaAs/AlGaAs interface, which can be seen from the spatial distribution of the carrier concentration in the conduction band simulated under higher gate voltages (1.1–1.4 V). When the gate voltage increases from –0.6 V to 1.4 V, both E_1 and E_2 decrease with different slopes in different gate voltage regions. In the region of –0.6 V to 0.2 V, both E_1 and E_2 decrease linearly with increasing gate voltage, with a slope of –0.13 and –0.214 for E_1 and E_2, respectively. These values correspond well with the geometric lever arms of l_1/l_0 (0.14) and l_2/l_0 (0.22), indicating that the simulation works very well for the sample structure. (The effective distance between the wetting layer and the back contact may be slightly different from the geometric value due to a spreading of charge from the back contact.)

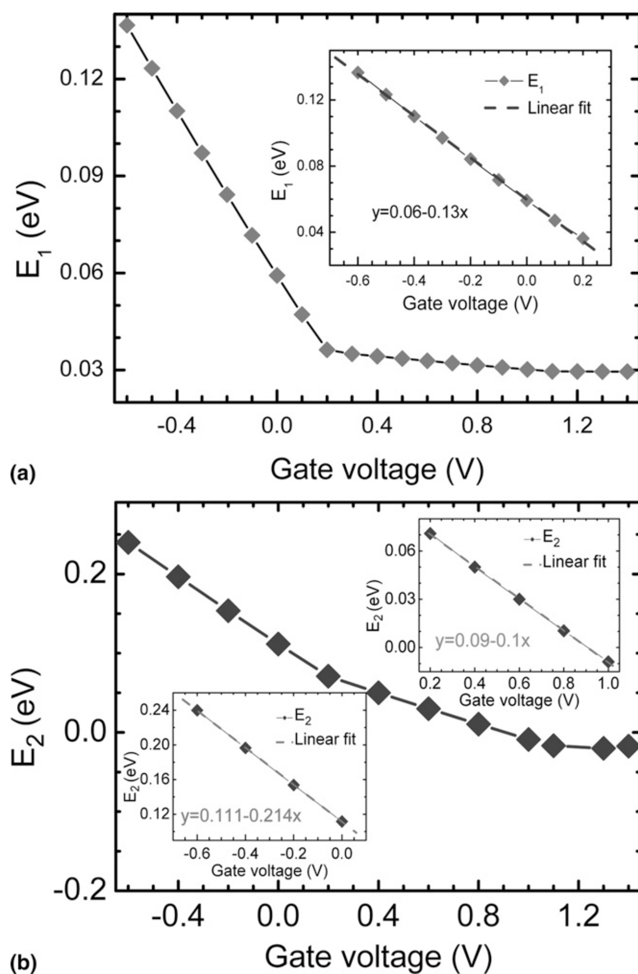

FIG. 4. The energies (a) E_1 and (b) E_2 as indicated in Fig. 1, calculated with different gate voltages. The inset of (a) shows a linear fit of E_1 in the range between –0.6 V and 0.2 V. The insets of (b) demonstrate the linear dependence of E_2 on V_g in the regions –0.6 V to 0.2 V and 0.2 V to 1.1 V.

As shown in Fig. 4, the linear lever arm approximation $E_2/E_1 = l_2/l_1$ holds up to the onset of the charging of the WL. Further, when the ground state of the WL is in resonance with the Fermi energy level, E_1 represents the energy difference between the ground state of the WL and the GaAs conduction band edge. When the gate voltage is increased further, the lever arm approximation ($E_2/E_1 = l_2/l_1$) cannot be used anymore, which can be seen from the small change of E_1 value when the gate voltage increases from 0.2 V to 1.1 V in the simulation. On the other hand, it is observed that when the gate voltage increases from 0.2 V to 1.1 V, E_2 also decreases linearly with increasing gate voltage. The slope of $E_2(V_g)$ in the region of 0.2 V to 1.1 V is –0.1, which is determined by sample structure, and can be used to extract E_2 when the WL is just charged in the C-V measurement [E_2(WL charging) = (1.8 – 0.9) × 0.1 = 0.09 eV]. Then, by using the linear lever arm $E_2/E_1 = l_2/l_1$ the energy difference between the electron ground state of WL and GaAs conduction band edge in the C-V measurements is determined to be 53 meV by assuming that the 2DEG is at the GaAs/AlGaAs interface. This, combined with the energy difference between the electron ground state of QDs and that of WL, and the ħω value obtained above, leads to the determination of the complete electron energy levels of QDs in the conduction band,[19] as shown in Fig. 5.

In the meantime, this 1D-Poisson/Schrödinger simulation is also performed on the sample studied by Granados and Garcia,[17] where the charging voltages of WL and 2DEG are taken to be 0.36 and 1.2 V, respectively. Further, the energy difference between the electron ground state of WL and the GaAs conduction band edge is extracted to be 56 meV, which is close to the number (55 meV) obtained by Granados and Garcia.[17] If the linear lever arm approximation holds up to the charging

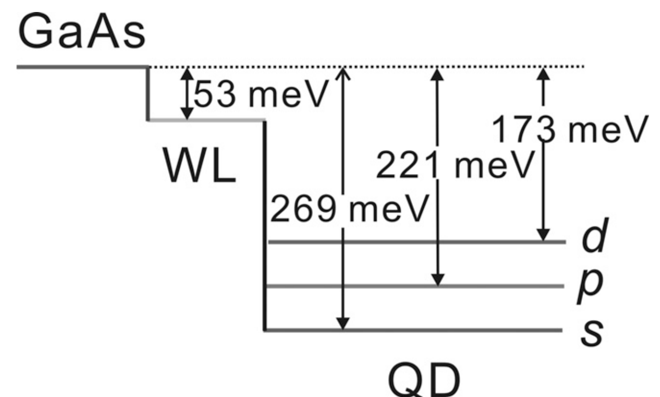

FIG. 5. Conduction band structure of the QD sample determined from C-V spectra and 1-D Poisson/Schrödinger numerical simulation.

of WL, the energetic distance from the energy levels in QDs and WL to GaAs conduction band edge produced by the method shown in this paper will be a close approximation to the corresponding numbers reported by Granados and Garcia.[17]

B. Electron energy levels in In(Ga)As/GaAs QRs

Though some experimental work has been done on the electronic structure of QDs, there is little data available about the energy structure of QRs.[2,22,23] C-V measurements and 1D Poisson/Schrödinger simulation are performed on the QR sample to probe the electron energy structure of the QRs.

A typical C-V spectrum of the QR sample taken at $f = 8113$ Hz and the second derivative of the C-V trace are shown in Fig. 6(a). The inset of Fig. 6(a) shows the typical AFM image of the sample surface. Obviously, In (Ga)As QRs are formed in the sample with a height of about 2 nm, an outer diameter of about 50 nm, and an inter diameter of about 20 nm. Clearly, at least four charging features can be observed in Fig. 6(a), which are labeled as s_1 (0.54 V), s_2 (0.804 V), WL (0.924 V), and 2DEG (1.828 V). Similar to the QD case, to extract the origin of these charging features, C-V measurements of the sample are also performed at different perpendicular magnetic fields, which range from 0 T to 11 T with an interval of 0.5 T. Figure 6(b) shows the C-V spectra of the sample taken at different perpendicular magnetic fields with $f = 8113$ Hz. According to the energy dispersion of these charging features, the charging peaks labeled s_1 and s_2 can be attributed to loading of the first and second electron into s-like states of the QRs.[2,24] Furthermore, the charging features labeled WL and 2DEG can be attributed to the loading of electrons into InAs WL and 2DEG, respectively.[16–19]

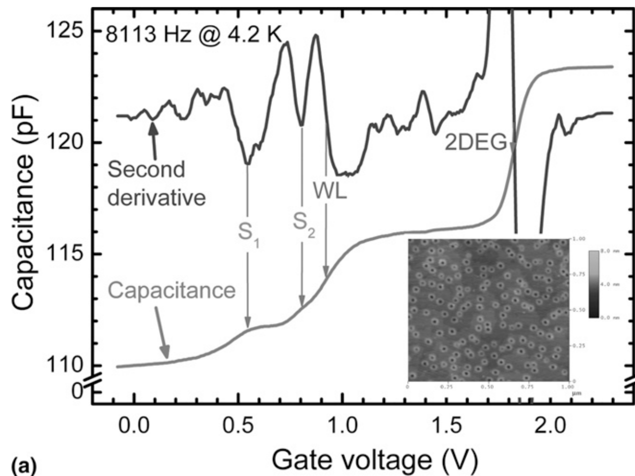

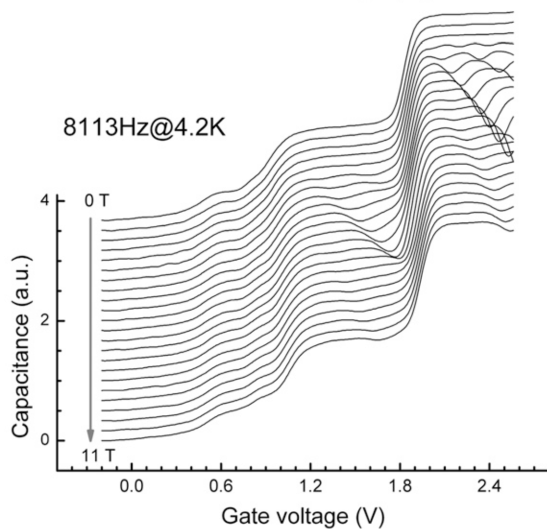

FIG. 6. (a) Typical C-V spectrum and its second derivative and (b) C-V spectra of the QR sample taken with $f = 8113$ Hz at different perpendicular magnetic fields that range from 0 T to 11 T with an interval of 0.5 T. The arrows in (a) mark the positions of the charging events. The inset of (a) shows a typical AFM image of the sample surface.

As discussed in Sec. III. A, it is also reasonable to use the linear lever arm approximation ($\Delta E = e\Delta Vg/\lambda$, with the lever arm $\lambda = l_0/l_1$) up to the charging of WL to convert charging voltages into charging energies, taking into account the low QR density ($\sim 1.56 \times 10^{10}$ cm^{-2}) grown in the sample. By using the linear lever arm approximation, the energy difference between the electron ground state of In(Ga)As QRs and the electron ground state of InAs WL can be determined to be ~48.5 meV.

To extract the energy difference between the ground state of WL and the GaAs conduction band edge, a 1D Poisson/Schrödinger simulation is also performed on the QR sample with different gate voltages. In the simulation, a 1.2 nm $In_{0.38}Ga_{0.62}As$ layer is used to represent the InAs WL. (The value of 1.2 nm $In_{0.38}Ga_{0.62}As$ as the InAs wetting layer was chosen to reproduce the 0.9 V gate voltage difference between the onset of the charging of the wetting layer and that of the 2DEG in the 1D Poisson/Schrödinger simulation.) The Schottky barrier on the sample surface and the Si-doping concentration in the back contact are also assumed to be 0.6 eV and 1×10^{18} cm^{-3}, respectively. In a similar manner, the energy difference between the electron ground state of WL and the GaAs conduction band edge in the QR sample is found to be 57 meV. Combined with the energy difference between the ground state of QRs and the ground state of WL extracted, the energy difference between the ground state of the QRs and the GaAs conduction band edge is determined to be 105 meV.

IV. CONCLUSIONS

In conclusion, C-V and one-dimensional numerical simulation using Poisson/Schrödinger equations are demonstrated as a simple and useful method to probe the energy structure of self-assembled nanostructures. By

using a linear lever arm approximation, the energy difference between the discrete energy levels in the nanostructures and the ground state of WL can be obtained directly from CV measurements. Meanwhile, the energetic distance from the ground state of WL to the GaAs conduction band edge can also be inferred indirectly from a 1D Poisson/Schrödinger simulation of the conduction band under different gate voltages, which results in the construction of the entire electron energy levels of the nanostructures in the conduction band.

ACKNOWLEDGMENTS

This work was supported by the Bundesministerium für Bildung und Forschung (01 BM 164 and 01 BM 451) and the Australian Research Council.

REFERENCES

1. D. Bimberg, M. Grundmann, and N.N. Ledentsov: *Quantum Dot Heterostructures* (John Wiley & Sons, New York, 1999).
2. A. Lorke, R.J. Luyken, A.O. Govorov, and J.P. Kotthaus: Spectroscopy of nanoscopic semiconductor rings. *Phys. Rev. Lett.* **84,** 2223 (2000).
3. N. Vukmirovi, D. Indjin, V.D. Jovanovi, Z. Ikoni, and P. Harrison: Symmetry of k·p Hamiltonian in pyramidal InAs/GaAs quantum dots: Application to the calculation of electronic structure. *Phys. Rev. B* **72,** 075356 (2005).
4. J.I. Climente, M. Korkusinski, M.F. Doty, M. Scheibner, A.S. Bracker, G. Goldoni, D. Gammon, and P. Hawrylak: Antibonding hole ground state in artificial molecules. *OAtube Nanotechnology* **1,** 901 (2008).
5. C. Tablero: Energy levels in self-assembled quantum arbitrarily shaped dots. *J. Chem. Phys.* **122,** 064701 (2005).
6. G.B. Ren and J.M. Rorison: Electronic structure of $In_{1-x}Ga_xAs$ quantum dots via finite difference time domain method. *Phys. Rev. B* **77,** 245318 (2008).
7. O. Voskoboynikov, Y. Li, H-M. Lu, C-F. Shih, and C.P. Lee: Energy states and magnetization in nanoscale quantum rings. *Phys. Rev. B* **66,** 155306 (2002).
8. J.I. Climente, J. Planelles, and F. Rajadell: Energy structure and far-infrared spectroscopy of two electrons in a self-assembled quantum ring. *J. Phys.: Condens. Matter* **17,** 1573 (2005).
9. S. Yamauchi, K. Komori, I. Morohashi, K. Goshima, and T. Sugaya: Electronic structures in single pair of InAs/GaAs coupled quantum dots with various interdot spacings. *J. Appl. Phys.* **99,** 033522 (2006).
10. L. Chu, A. Zrenner, G. Böhm, and G. Abstreiter: Lateral intersubband photocurrent spectroscopy on InAs/GaAs quantum dots. *Appl. Phys. Lett.* **76,** 1944 (2000).
11. O. Engström and M. Kaniewska: Deep level transient spectroscopy in quantum dot characterization. *Nanoscale Res. Lett.* **3,** 179 (2008).
12. D. Reuter: Capacitance-voltage spectroscopy of InAs quantum dots, in *Self-Assembled Quantum Dots*, edited by Z.M. Wang (Springer, New York, 2008).
13. H. Drexler, D. Leonard, W. Hansen, J.P. Kotthaus, and P.M. Petroff: Spectroscopy of quantum levels in charge-tunable InGaAs quantum dots. *Phys. Rev. Lett.* **73,** 2252 (1994).
14. G. Medeiros-Ribeiro, D. Leonard, and P.M. Petroff: Electron and hole energy levels in InAs self-assembled quantum dots. *Appl. Phys. Lett.* **66,** 1767 (1995).
15. M. Fricke, A. Lorke, J.P. Kotthaus, G. Medeiros-Ribeiro, and P.M. Petroff: Shell structure and electron-electron interaction in self-assembled InAs quantum dots. *Europhys. Lett.* **36,** 197 (1996).
16. C. Bock, K.H. Schmidt, U. Kunze, S. Malzer, and G.H. Döhler: Valence-band structure of self-assembled InAs quantum dots studied by capacitance spectroscopy. *Appl. Phys. Lett.* **82,** 2071 (2003).
17. D. Granados and J.M. Garcia: Determination of the energy levels on InAs quantum dots with respect to the GaAs conduction band. *Nanotechnology* **16,** s282 (2005).
18. S. Tarucha, D.G. Austing, T. Honda, R.J. van der Hage, and L.P. Kouwenhoven: Shell filling and spin effects in a few electron quantum dot. *Phys. Rev. Lett.* **77,** 3613 (1996).
19. R.J. Warburton, B.T. Miller, C.S. Dürr, C. Bödefeld, K. Karrai, and J.P. Kotthaus: Coulomb interactions in small charge-tunable quantum dots: A simple model. *Phys. Rev. B* **58,** 16221 (1998).
20. R.J. Luyken, A. Lorke, A.O. Govorov, J.P. Kotthaus, G. Medeiros-Ribeiro, and P.M. Petroff: The dynamics of tunneling into self-assembled InAs dots. *Appl. Phys. Lett.* **74,** 2486 (1999).
21. G.L. Snider: *Computer Program 1D Poisson/Schrödinger: A Band Diagram Calculator* (http://www.nd.edu/~gsnider, University of Notre Dame, IN).
22. R.J. Warburton, C. Schaflein, D. Haft, F. Bickel, A. Lorke, K. Karrai, J.M. Garcia, W. Schoenfeld, and P.M. Petroff: Optical emission from a charge-tunable quantum ring. *Nature* **405,** 926 (2000).
23. S. Sanguinetti, M. Abbarchi, A. Vinattieri, M. Zamfirescu, M. Gurioli, T. Mano, T. Kuroda, and N. Koguchi: Carrier dynamics in individual concentric quantum rings: Photoluminescence measurements. *Phys. Rev. B* **77,** 125404 (2008).
24. I. Filikhin, V.M. Suslov, and B. Vlahovic: Modeling of InAs/GaAs quantum ring capacitance spectroscopy in the nonparabolic approximation. *Phys. Rev. B* **73,** 205332 (2006).